Vol. 79: 63–75, 2019
https://doi.org/10.3354/cr01578

CLIMATE RESEARCH
Clim Res

Published online November 14

Variability of heat waves and recurrence probability of the severe 2003 and 2013 heat waves in Zhejiang Province, southeast China

Weiping Lou[1,*], Yiping Yao[2], Ke Sun[1], Shengrong Deng[1], Ming Yang[1]

[1]Xinchang Weather Bureau, Xinchang County 312500, Zhejiang Province, PR China
[2]Zhejiang Climate Center, Hangzhou 310017, PR China

ABSTRACT: Summer heat wave (HW) events have disastrous consequences for human health, economies, and ecosystems. The present study investigates the variability of HWs and estimates the recurrence probabilities of the severe 2003 and 2013 hot summers in Zhejiang Province, southeast China. We define a HW event as ≥3 consecutive days having a daily maximum temperature ≥35°C. Considering this definition, 2 HW indices were adopted: the yearly sum of accumulated harmful high temperature (YAHHT) of HWs and the yearly sum of HW duration (HWD). We found that the YAHHT and HWD have had significant increasing trends in the majority of Zhejiang. The inter-annual variability of HWs can be divided into 3 periods: 1973–1987, 1988–2002, and 2003–2017. The severity levels of HWs in Zhejiang had a clearly increasing trend according to the YAHHT and HWD. The average YAHHT and HWD in 2003–2017 were, respectively, >2.0 and >1.5 times those in 1973–1987 and 1988–2002. We also estimated the recurrence probabilities of the HWs that occurred in Zhejiang during July–September 2003 and 2013. The recurrence probabilities of such severe HWs, which were assessed in simulations using an information diffusion model, are higher in the present climate.

KEY WORDS: Variability · Recurrence probability · Accumulated harmful high temperature of heat waves · Information diffusion model

1. INTRODUCTION

Heat wave (HW) events affect the environment and society (Spinoni et al. 2015), often via disasters affecting ecosystems and human society in terms of health, energy supply, hydrology, forestry, and agriculture (e.g. Savić et al. 2014, Roldán et al. 2016, Prasad & Jagadish 2017).

Although no universal definition for HWs has been adopted (Unal et al. 2013), there are some principles that are usually applied. In general, HWs are defined by (1) a temperature indicator (e.g. daily average, maximum, or minimum temperature), (2) a temperature threshold (i.e. a relative or absolute threshold), and (3) duration (Smith et al. 2013). In the past few years, several climate indices have been applied to quantify the duration and severity of HWs on the basis of nighttime minima or daytime maxima (Russo et al. 2015). However, all of these indices have limited robustness when applied to compare the severity of HWs across regions and times. Most of the defined HW indices tend to be constructed with a certain impact group or sector (e.g. human health, wildlife, agriculture, bushfire/wildfire, management, transport, and energy supply) in mind and, owing to their complexity, they may not be transferable and comparable across regions, time periods, or between population groups (Perkins 2015, Russo et al. 2015). For exam-

*Corresponding author: xclwp@163.com

ple, on the basis of climate change and adaptation strategies for human health and improving public health responses to extreme weather/HWs, the World Meteorological Organization defines a HW as a period of ≥5 consecutive days with the daily maximum temperature exceeding the average maximum temperature by 5°C or more (WMO & WHO 2015). Considering the effects of HWs on mortality in The Netherlands, the Netherlands Royal Meteorological Institute defines a HW as a period of ≥5 consecutive days with daily maximum temperature values of ≥25°C, including ≥3 days with maximum temperatures of ≥30°C (Huynen et al. 2001). In order to evaluate the temporal distribution of surface atmospheric water vapor levels during short-duration extreme heat events in Chicago (USA), Changnon et al. (2003) defined a HW as a period of ≥3 consecutive days with maximum (minimum) temperature levels >35°C (24°C). To assess the effect of HWs on tea production in Zhejiang Province (China), Lou et al. (2018) defined a HW as a period of ≥4 consecutive days characterized by an average temperature >30°C, a maximum temperature >35°C, and levels of relative humidity <65%. In China, when the daily maximum temperature during 3 consecutive days >35°C, meteorological stations are required to issue high-temperature warnings to the public.

Zhejiang is an area in China frequently affected by HWs (Ye et al. 2013). However, there is still a lack of research on the temporal and spatial variation features of HWs over this particular region. HW activity has regional characteristics (Gross et al. 2017). In highly urbanized areas, one adverse result of urbanization is the urban heat island effect, wherein a combination of various factors renders the temperature levels within the urban region higher than those experienced over the more rural and vegetated surrounding areas (Lee & Ho 2010, Peres et al. 2018). Urbanization changes the atmospheric dynamics, and heat modifies the properties of the underlying surface in cities. The urban heat island effect strengthens with the size of the city and population. The release of artificial heat from factories, mines, enterprises, government departments, and the daily activities of urban residents also enhance the urban heat island effect (Shou & Zhang 2012). Different urbanization processes and the development of heat islands have distinct effects on the HW development in different areas of Zhejiang (Yang et al. 2011).

With increasing mean temperatures, HWs will not only become more frequent, but their duration and intensity are also likely to increase (IPCC 2014). According to IPCC AR5, the annual average temperature has increased at 0.23°C decade^{-1} since the 1970s in China. In Zhejiang, summer and annual average temperatures have respectively increased 0.30 and 0.34°C decade^{-1} (Lou et al. 2017). HWs have represented a serious natural hazard in Zhejiang since 2003 (Sun et al. 2014, Wang et al. 2016). It is therefore necessary to carry out further research on changes in HW activity in Zhejiang, given that systematic research on this climatic subject is lacking for this region in particular. Within this context, the present study should be used by authorities as a basis for research on HW prevention in order to mitigate the already known impacts for human health, agricultural production, and ecosystems.

The duration (number of HW days) and intensity are important characteristics of a HW (Perkins & Alexander 2013). There are several indices that represent the intensity of HWs (Perkins 2015). Heat-related damage (e.g. metabolic, circulatory and respiratory illnesses, crop failures, power outages, wildfires) may occur not only due to intense heat exposure during a sporadic single day, but also due to accumulated heat stress over a longer period (Tan & Huang 2004, Nogueira & Paixão 2008, Lee et al. 2016, Siegle et al. 2018). In this study, appropriate metrics were used to detect and quantify changes in HW duration and intensity that occurred during the defined extended summer period (i.e. June–September) in Zhejiang. In order to provide a scientific basis for mitigating the impacts of severe HW episodes in the future, we also computed and analyzed the recurrence probability of historical severe HW episodes that occurred during the hot summer periods of 2003 and 2013 (Sun et al. 2014, Xia et al. 2016).

2. MATERIALS AND METHODS

2.1. Data

Data were obtained from 75 stations located within urban areas across Zhejiang, which is one of the most economically developed provinces in China (Jiang et al. 2018) and is prone to severe HWs. Originally, the data were provided by the Network Center of the Zhejiang Provincial Meteorological Bureau (NCZP). The NCZP checked and controlled all datasets for quality and homogeneity, adopting the cumulative deviation test and the standard normal homogeneity test (Lou et al. 2017). The NCZP provided hourly temperatures and daily maximum temperatures. Of the 75 total stations from which data were obtained,

only 67 with continuous time series (i.e. no data gaps) from 1 January 1973 to 31 December 2017 were used in the present study (Fig. 1).

All 67 stations were located within an urban environment, so they were aggregated into 4 city groups. The groups were classified according to the nonagricultural population index (NAP), whose values were obtained from the China City Statistical Yearbook. The resulting groups were: (1) small cities with a NAP of 0.01–0.1 million people, (2) medium-sized cities with a NAP of 0.1–0.5 million people, (3) large cities with a NAP of 0.5–1.0 million people, and (4) metropolises with a NAP of over 1.0 million people (Yang et al. 2011). We used data from 31 medium-sized-city stations (MCSs) and 32 small-city stations (SCSs). Wenzhou and Shaoxing stations are large-city stations (LCSs) while Hangzhou and Ningbo stations are metropolitan stations (MESs) (Fig. 1).

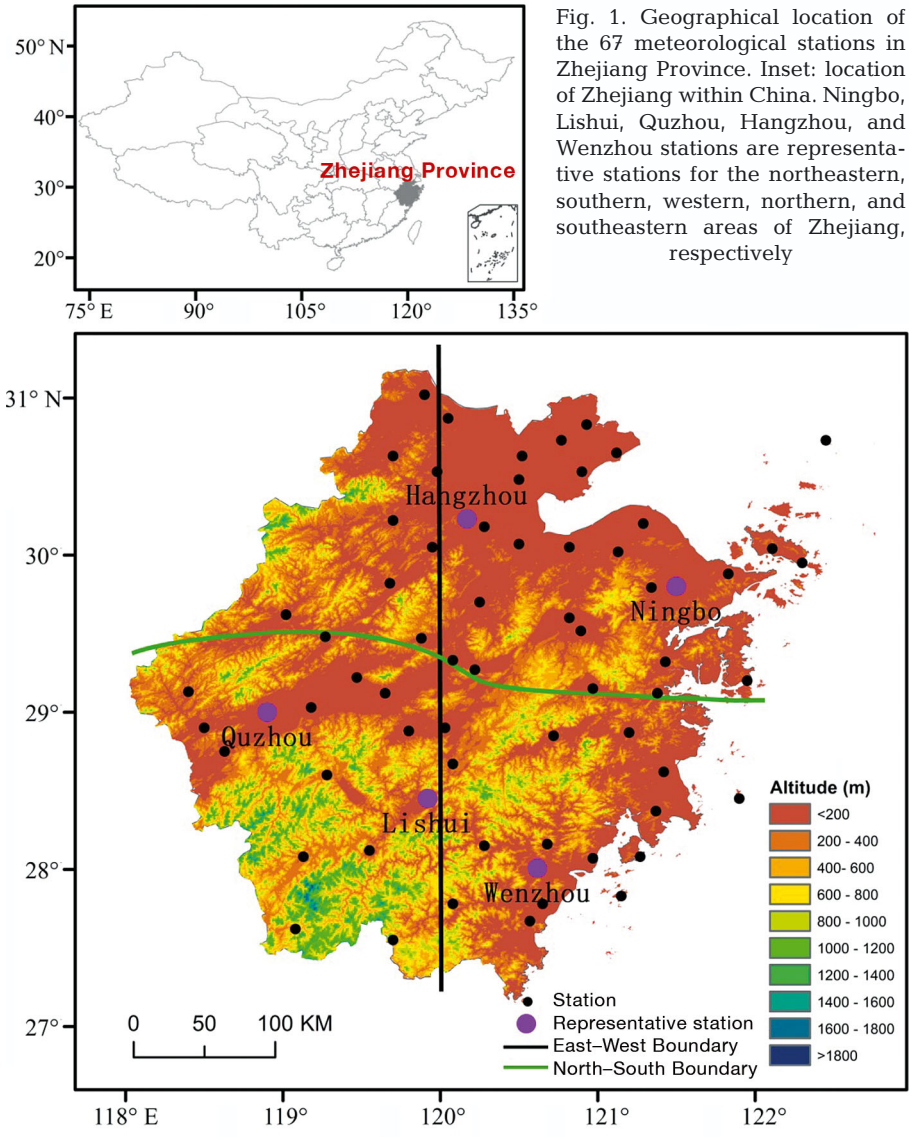

Fig. 1. Geographical location of the 67 meteorological stations in Zhejiang Province. Inset: location of Zhejiang within China. Ningbo, Lishui, Quzhou, Hangzhou, and Wenzhou stations are representative stations for the northeastern, southern, western, northern, and southeastern areas of Zhejiang, respectively

Furthermore, the distance of each continental station from the sea (DCS) was calculated according to a 1:250 000 digital elevation model and geographic information system. Table A1 in the Appendix presents the 67 stations used in the analysis of the variability of HWs, including the station IDs, names, geographical coordinates, elevations, types, and DCSs.

The province is divided into northern and southern areas using the north–central subtropical boundary of the climate zoning map of Zhejiang (green line in Fig. 1). The mainland of Zhejiang lies between 118 and 122° E. The longitude of 120° E (black line in Fig. 1) divides Zhejiang into eastern and western areas (Zhang & Guo 1999).

Hangzhou station is located in the Hangjiahu Plain, northern Zhejiang. Hangzhou is the capital city of Zhejiang Province and is one of the central cities of urban agglomeration in the Yangtze River Delta. Ningbo station is located in a hilly area of northeast Zhejiang. Although it is located 25.76 km from the coastline, the Zhoushan Islands lie between the East China Sea and Ningbo. Wenzhou station is located 16.95 km from the coastline, on the Wenrui Plain, southeast Zhejiang. Lishui station is located in the southern region of Zhejiang, more specifically in the Lishui Basin, which encompasses an area of about 36 km^2 surrounded by mountains. Quzhou station is located in the Jinqu Basin, western Zhejiang. We use the names Ningbo, Lishui, Quzhou, Hangzhou, and Wenzhou to refer to the northeastern, southern, western, northern, and southeastern areas of Zhejiang, respectively.

2.2. Methodology

2.2.1. HW definition and characterization

A HW is generally defined as a relatively long period of consecutive days with extremely hot conditions. According to this general definition, a wide variety of methods, largely described in the scientific literature, have been devel-

oped to quantify HWs and their variables (Perkins 2015, WMO & WHO 2015). Several HW definitions, such as the one adopted in this study, use an absolute threshold methodology to define a HW as a period characterized by temperature values above a constant threshold. Such a methodology should be adopted when the analysis is carried out with a particular sector in mind and for a specific region where the impacts of extreme heat-stress conditions on natural–human environments are exacerbated when temperature values surpass an absolute defined level. Particularly for Zhejiang Province, many studies have shown that HWs strongly affect agriculture, forestry, animal husbandry, and fisheries, especially when temperature levels exceed 35°C. The growth and yield of the main crops grown in this region (rice, maize, tea, and citrus) are strongly affected when temperatures rise above this threshold (Feng et al. 2008, Lou et al. 2010, 2018). The Ministry of Human Resources and Social Security of China stipulates that employers must pay high-temperature allowances to workers who work outdoors during days with a daily maximum temperature higher than 35°C (Xie 2017). The China Meteorological Administration (CMA) defines extreme temperature as a daily maximum temperature >35°C and a HW as a period of ≥3 consecutive days with a daily maximum temperature ≥35°C (Xu et al. 2009). Taking into account the previous considerations, we used the CMA definition of HW in this analysis.

The effects of HWs on the environment and society mainly result from the accumulative effects of harmful high temperatures (i.e. the cumulative value of the partial temperature above a temperature threshold) (Nogueira & Paixão 2008, Feng et al. 2015, Lee et al. 2016). The present paper defines the accumulated harmful high temperature (AHHT) of a HW as the accumulated value of the partial temperature above a threshold during a HW event. The AHHT is presented as a useful index to evaluate the HW magnitude and is computed as:

$$\begin{aligned} \mathrm{AHHT} &= \int_{j=1}^{j=n}\int_{t=0}^{t=24}[T_{j,t}-35]\,\mathrm{d}t\,\mathrm{d}j \\ &= \sum_{j=1}^{n}\sum_{t=1}^{24}(T_{j,t}-35) \end{aligned} \quad (1)$$

where n is the HW duration (days), $T_{j,t}$ is the temperature (°C) at hour t of the j^{th} HW calendar day. $T_{j,t}$ – 35 assumes a value of 0 if $T_{j,t} < 35$°C.

Two yearly indices were computed and analyzed to characterize HWs in terms of their duration and intensity: (1) the yearly AHHT (YAHHT), which is the annual sum of all daily AHHT values calculated for each HW, and (2) the yearly HW duration (HWD), which is the annual sum of all days that were considered part of the HW (Perkins & Alexander 2013). The values of the AHHT and HWD indices were computed only for the days within the extended summer period (June–September).

The AHHT index, defined as the cumulative value of the partial temperature above a temperature threshold, depends on 2 distinct aspects: (1) the induced heat-stress conditions and their anomalies regarding the expected values during days under a HW regime; (2) the total number of days under a HW regime. By normalizing the YAHHT by the HWD (YAHHT/HWD), we obtain a variable whose values depend exclusively on the yearly heat-stress conditions induced by the occurrence of n HW events and not from the total yearly HW days. Thus, the YAHHT/HWD parameter quantifies the average values of the partial hourly temperature above 35°C for all annual n HW days.

An extreme climatic event implies the occurrence of a severe meteorological scenario affecting a relatively large area and throughout a relatively long period. The longest event might occur over a small area, while events affecting a large area might be below an intensity criterion. The severity of annual hot summers could be evaluated considering the duration, extent, and intensity of all summer HW episodes in terms of the induced heat-stress levels. The average HWD of all stations affected by all summer HW episodes is used as the duration criterion, the maximum number of stations affected by all the summer HW episodes is used as the extent criterion, and the average YAHHT/HWD of all stations affected by all summer HW episodes is used as the intensity criterion. To measure the hot summer severity considering the above mentioned aspects, the comprehensive index (Ci) is constructed as:

$$Ci = a_1 \times F_1 + a_2 \times F_2 + a_3 \times F_3 \quad (2)$$

where F_1, F_2, and F_3 are respectively the standardized average HWD of all stations, the maximum number of stations affected by all summer HW episodes, and the average YAHHT/HWD of all stations affected by all summer HW episodes, while a_1, a_2, and a_3 are their corresponding coefficients (Ding & Ke 2015). The importance and the degree of abnormality of each index may be different. The present study applies the method recommended by Ren et al. (2012) to calculate the weight coefficients for the duration index, extent index, and intensity index, whose values were 0.3248, 0.3040, and 0.3712 respectively.

2.2.2. Trend analysis

Sen's slope estimator method is a nonparametric test developed by Sen (1968) to estimate the true slope of Mann–Kendall's trend analysis for a sample of N pairs of data (Shadmani & Roknian 2012). This estimator has been widely used in meteorological time series (Raggad 2018), so we used this statistical method to verify the presence of trends with statistical significance at the 95% confidence level.

A moving *t*-test was performed to detect the mutation feature of the *Ci* series (Liu & Xu 2016). A Student's *t*-test was conducted to compare data changes between different periods (Hellebrekers et al. 1997, Lou et al. 2017). For both of these statistical analyses, we used a significance level (α) of 0.05.

2.2.3. Risk assessment model for HWs

The information diffusion model falls within the scope of fuzzy mathematics, and is used to handle a data sample with incomplete information (Huang 1997). The method is based on retaining the raw information of the data to a great extent and translating the information into a fuzzy relation to skirt calculating a membership function (Huang 2002). Let $Y = \{y_1, y_2, y_3 \ldots, y_n\}$ be a set of observations and $U = \{u_1, u_2, u_3 \ldots u_m\}$ be the chosen framework space. If the observations are not able to provide sufficient information to identify the precise relationship that is needed, then Y is called an incomplete data set. For any $y \in Y$ and $u \in U$, Eq. (3) describes normal information diffusion:

$$f_j(u_i) = \frac{1}{h \cdot \sqrt{2\pi}} \cdot \exp\left[-\frac{(y_j - u_i)^2}{2h^2}\right] \quad (3)$$

where $f_j(u_i)$ is information diffusion function which spreads y_j information to u_i, y_j and u_i are respectively a given sample and the controlling points. The universe U is the monitoring space, and h is the diffusion coefficient, calculated on the basis of Table 1.

It is assumed that:

$$C_j = \sum_{i=1}^{m} [f_j(u_i)] \quad (4)$$

C_j is the sum of the information that y_j diffuse to all u.

The membership function of the fuzzy subset is:

$$\mu_{y_j}(u_i) = f_j(u_i) / C_j \quad (5)$$

where $\mu_{y_j}(u_i)$ is the normalizing information distribution of sample y_j.

Table 1. Relationship between the number of samples (n) and diffusion coefficient (h), which is applied in Eq. (3). b and a: maximum and minimum values, respectively, for the samples

n	h
5	$0.8146(b-a)$
6	$0.5690(b-a)$
7	$0.4560(b-a)$
8	$0.3860(b-a)$
9	$0.3362(b-a)$
10	$0.2986(b-a)$
≥11	$2.6851(b-a)/(n-1)$

It is further assumed that:

$$q(u_i) = \sum_{j=1}^{n} [\mu_{y_j}(u_i)] \quad (6)$$

The physical meaning of Eq. (6) is that if the observation values can only be chosen as one of the values in the series of $u_1, u_2, \ldots, u_m$ then the sample number with the observation value of u_i can be determined to be $q(u_i)$ through the information diffusion from the observation set of $y_1, y_2, \ldots, y_n$, in regards to all values of y_j as the representatives of the samples. It is clear that the value of $q(u_i)$ is generally not a positive integer, but it is certain to be a number no less than zero.

The probability of u_i is calculated as:

$$P(u_i) = q(u_i) / \sum_{i=1}^{m} [q(u_i)] \quad (7)$$

and the exceedance probability $[P(u \geq u_i)]$ of u_i is calculated as:

$$P(u \geq u_i) = \sum_{k=i}^{m} u_k \quad (8)$$

The present study applies the information diffusion model to calculate the recurrence probability of a severe HW in different periods.

3. RESULTS

3.1. Trends of HWs

Trend values were computed for the YAHHT, HWD, and YAHHT/HWD index levels and for the period 1973–2017 (Fig. 2). Most of the stations located throughout the eastern coastal region recorded low and statistically non-significant trend values. The same was observed for the stations located within the northeastern islands. For both regions, the ocean effect may have been preponderant to obtain such low trend values, by reducing the

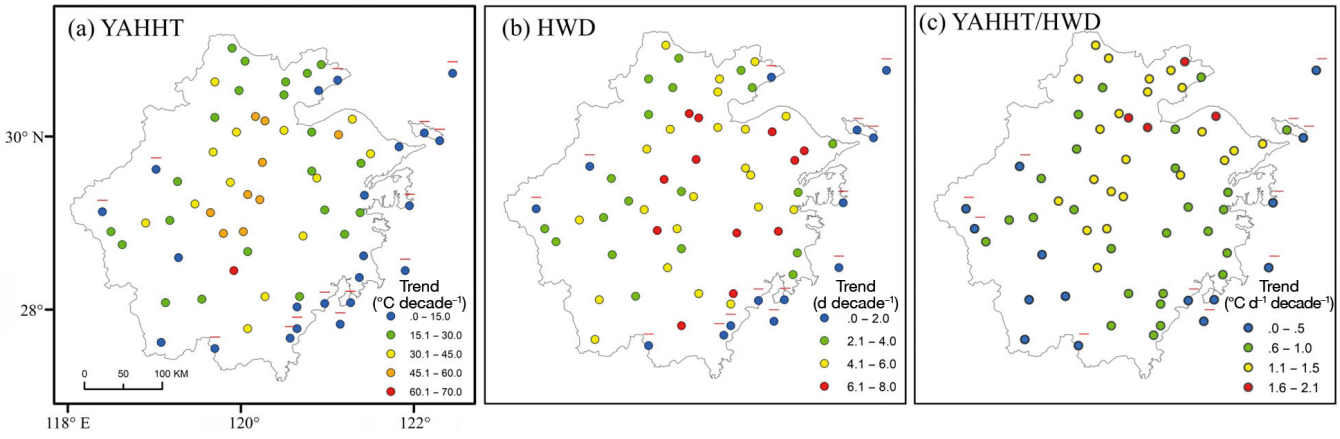

Fig. 2. Spatial distributions of (a) yearly accumulated harmful high temperature (YAHHT), (b) heat wave duration (HWD), and (c) YAHHT/HWD trends during 1973–2017. Horizontal line above stations: trend not significant at the 5% significance level

days with daily maximum temperature ≥35°C, and so promoting an absence of significant HW episodes. In addition to these stations, low and statistically non-significant trend values were also observed for Chunan, Kaihua, and Taishun stations, which are surrounded by mountains with a pronounced forest coverage. Statistically significant trend values ($p \leq 0.05$) for the YAHHT, HWD, and YAHHT/HWD indices were recorded throughout most of the remaining stations (Fig. 2). The YAHHT trend was ≥30.1°C decade^{-1} at 23 stations while the HWD trend was ≥4.1 d decade^{-1} at 34 stations. The YAHHT/HWD trend was ≥1.1°C d^{-1} decade^{-1} at 26 stations.

Most stations with the YAHHT trend value above 30.0°C decade^{-1} were located between Hangzhou, Ninbo, Lishui, and Quzhou. Lishui station had the strongest YAHHT trend of 70°C decade^{-1}. In this area, the HWD and YAHHT/HWD trend values of most stations were respectively ≥4.1 d decade^{-1} and 1.1°C d^{-1} decade^{-1}. We therefore conclude that the YAHHT increase was due both to an enhancement of the heat-stress conditions and to an increment in the number of days under a HW regime. In the area between Ninbo and Wenzhou, the HWD trend values of most stations were ≥4.1 d decade^{-1}, and the YAHHT/HWD trend values were ≤1.0°C d^{-1} decade^{-1}. Thus we conclude that the YAHHT increase was mainly due to an increment in the number of days under a HW regime. In the north of Hangzhou, the YAHHT/HWD trend values of most stations were ≥1.1°C d^{-1} decade^{-1}, which indicates that the mean induced heat-stress conditions (HW intensity) have increased throughout the analysis period.

3.2. Stages of the long-term variability of HWs

Hot summers with *Ci* values <–0.5σ (where σ denotes a standard deviation) and >+0.5σ were respectively grouped as weak and strong hot summers, while those with *Ci* values be-tween –0.5σ and +0.5σ were classified as moderate (Ding & Ke 2015). In the present sudy, the *Ci* values for distinguishing strong, moderate, and weak hot summers were +0.4696 and –0.4696. Temporal variations of strong, moderate, and weak hot summers are given in Fig. 3. Of the 13 strong hot summers, 10 occurred during the period 2003–2017. The peak *Ci* values appeared in 2013 and secondly in 2003, indicating that the hot summers in these 2 years were the strongest and second strongest. The third and fourth strongest hot summers were in 2017 and 2007. Three strong hot summers occurred in 1988–2002. Moderate and weak hot summers occurred mainly in 1973–2002. Among them, 8 weak and 7 moderate hot summers occurred in 1973–1987. The weakest hot summer occurred in 1982. The second and third weakest hot summers were in 1997 and 1999.

The 8 yr moving average method was used to analyze the *Ci* time series, as shown in Fig. 4a. There was a stage-change relationship between *Ci* and time. The moving *t*-test showed that the *Ci* had 2 significant mutations, one in 1987 and the other in 2002 (Fig. 4b), and the 8 yr moving average value of *Ci* showed an upward trend after 1987 and 2002. To compare the characteristics of HWs in different stages, the YAHHT series and HWD series were divided into 3 periods: 1973–1987, 1988–2002, and 2003–2017. Student's *t*-test showed that the average values of the YAHHT and HWD in 2003–2017 were

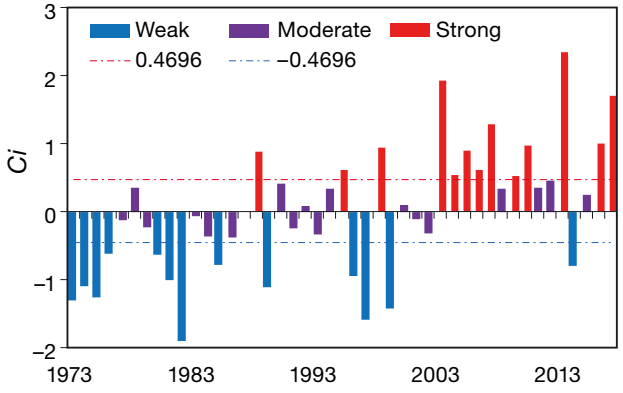

Fig. 3. Temporal variation in the comprehensive index of hot summer severity, *Ci*. For details on the index calculation, see Section 2.2.1

significantly higher than those in 1973–1987 and 1988–2002, and those in 1988–2002 were significantly higher than those in 1973–1987. The YAHHT average value in 2003–2017 was 4.6 times higher than in 1973–1987 and 2.3 times higher than in 1988–2002. The HWD average value in 2003–2017 was 2.3 times higher than in 1973–1987 and 1.6 times higher than in 1988–2002.

During 1973–1987, YAHHT values >100°C were only recorded for 4 stations, and 2 stations had average HWDs >30.0 d. During 1988–2002, there were 19 stations whose average YAHHT levels were >100°C, and 4 stations whose average HWD values were >30.0 d. During 2003–2017, there were 47, 25, and 6 stations whose average YAHHTs were >100, >200, and >300°C, respectively, with the maximum YAHHT being 407.7°C at Lishui station. We also identified 31 and 7 stations whose average HWDs were >30.0 and >40.0 d, respectively, with the maximum HWD being 49.1 d at Lishui station (Figs. 5 & 6).

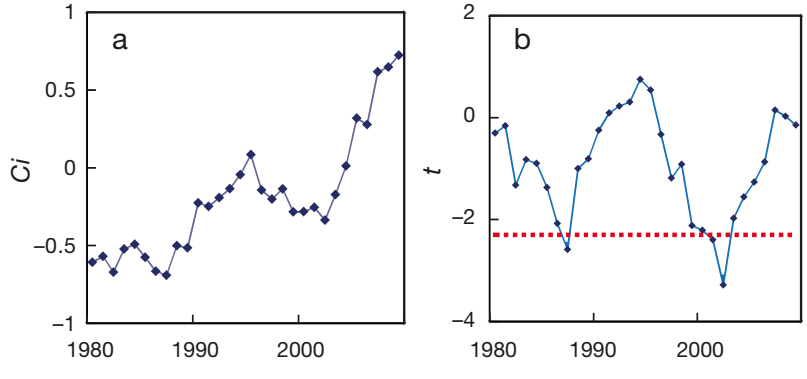

Fig. 4. (a) 8 yr moving average and (b) moving *t*-test of the comprehensive index of hot summer severity (*Ci*) time series. In (b), the solid line shows the *t*-value, and the red dashed line shows statistical significance at the 95% confidence level

3.3. Recurrence probability of the severe 2003 and 2013 HWs

Ningbo, Lishui, Quzhou, Hangzhou, and Wenzhou stations are respectively located in the northeastern, southern, western, northern, and southeastern areas of Zhejiang. We will focus in detail on the most severe HWs recorded simultaneously throughout the 5 locations. Over the period of available data (1973–2017), the hot period from 1 July to 18 August 2013 was the most extreme hot summer in Zhejiang (Fig. 3). The average YAHHT and HWD of all 67 stations were respectively 487.6°C and 39.7 d. During 2013, 62 meteorological stations recorded HWs, and 35 stations verified their record highest temperatures since the beginning of their records. The most extreme daily maximum temperature of 44.1°C occurred on 11 August at Xinchang station. This was the highest recorded value among all meteorological stations in Zhejiang since their establishment. Here we present Hangzhou and Lishui stations as examples. At Hangzhou, during the period from 24 to 30 July 2013 (7 consecutive days) and during the period from 5 to 12 August (8 consecutive days), daily maximum temperatures exceeded 40°C. On 9 August, a daily maximum temperature of 41.6°C was observed, a value that established a new historical record for this particular station. The HWs from 1 July to 18 August were also recorded at Lishui station, where the highest daily maximum temperature of 41.8°C was recorded on 8 August. Lishui also recorded HWs from 23 to 29 August and from 9 to 13 September.

The July–September 2003 hot period was the second most severe hot summer in Zhejiang. The average YAHHT and HWD for all stations were respectively 397.9°C and 39.3 d. In 2003, HWs were recorded at 62 stations. The highest recorded temperature was 43.2°C, observed on 31 July at Lishui station. There were 3 phases of HWs: July to early August, late August, and early September. Hangzhou station recorded HWs during the periods of 12 July to 8 August, 22 to 30 August, and 3 to 7 September. The highest daily maximum temperature of 40.3°C occurred on 1 August. Lishui station recorded HWs during the periods of 29 June to 11 August, 22 to 31 August, and 5 to 9 September, and a maximum temperature ≥40°C on 14 d.

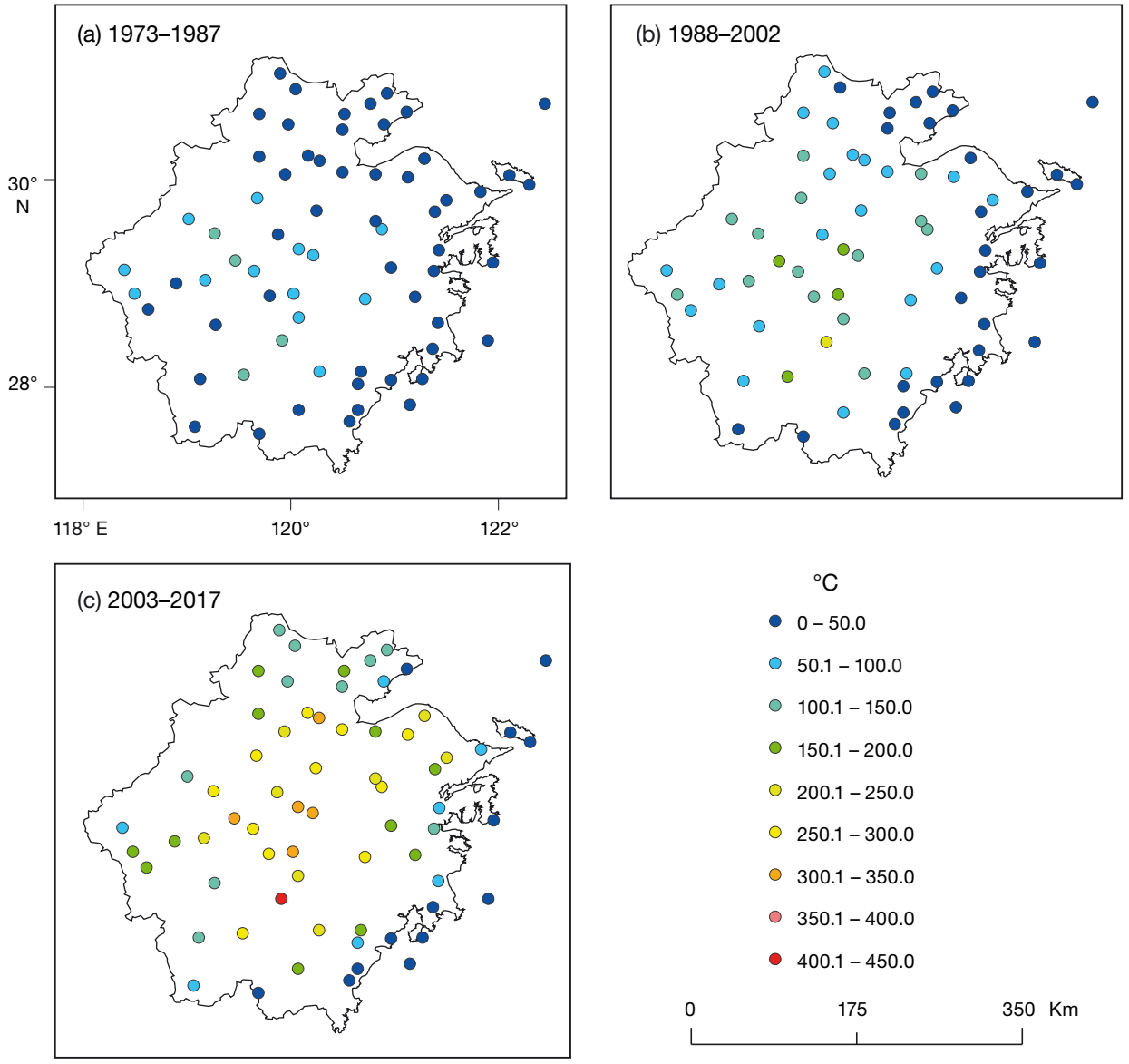

Fig. 5. Yearly accumulated harmful high temperature (YAHHT) average values recorded for the periods (a) 1973–1987, (b) 1988–2002, and (c) 2003–2017

Table 2 presents the recurrence probabilities of the 2003 and 2013 YAHHT values for the periods of 1973–1987, 1988–2002 and 2003–2017, for Hangzhou, Ningbo, Quzhou, Lishui, and Wenzhou stations. During both 1973–1987 and 1988–2002, none of these 5 stations recorded YAHHT values similar to the ones observed during 2003 and 2013 (Table 2). In fact, the highest observed YAHHT during these 2 periods, which were all recorded in 1988, were much lower than those verified for the years 2003 and 2017 (Hangzhou: 197.9°C; Ningbo: 174.8°C; Quzhou: 233.1°C; Lishui: 487.5°C; Wenzhou: 66.1°C). However, throughout the present climate (2003–2017) and for all stations, extreme YAHHT values similar to those recorded in 2003 and 2017 were verified regularly during several years. YAHHT values, such as the ones recorded in 2003, had a recurrence probability of 18.7, 16.4, 9.1, 3.3 and 7.2% in Hangzhou, Ningbo, Quzhou, Lishui, and Wenzhou, respectively. Regarding the 2013 YAHHT value, the recurrence probabilities for the present climate are 3.4, 3.5, 4.4, 10.2, and 9.5% for Hangzhou, Ningbo, Quzhou, Lishui, and Wenzhou, respectively.

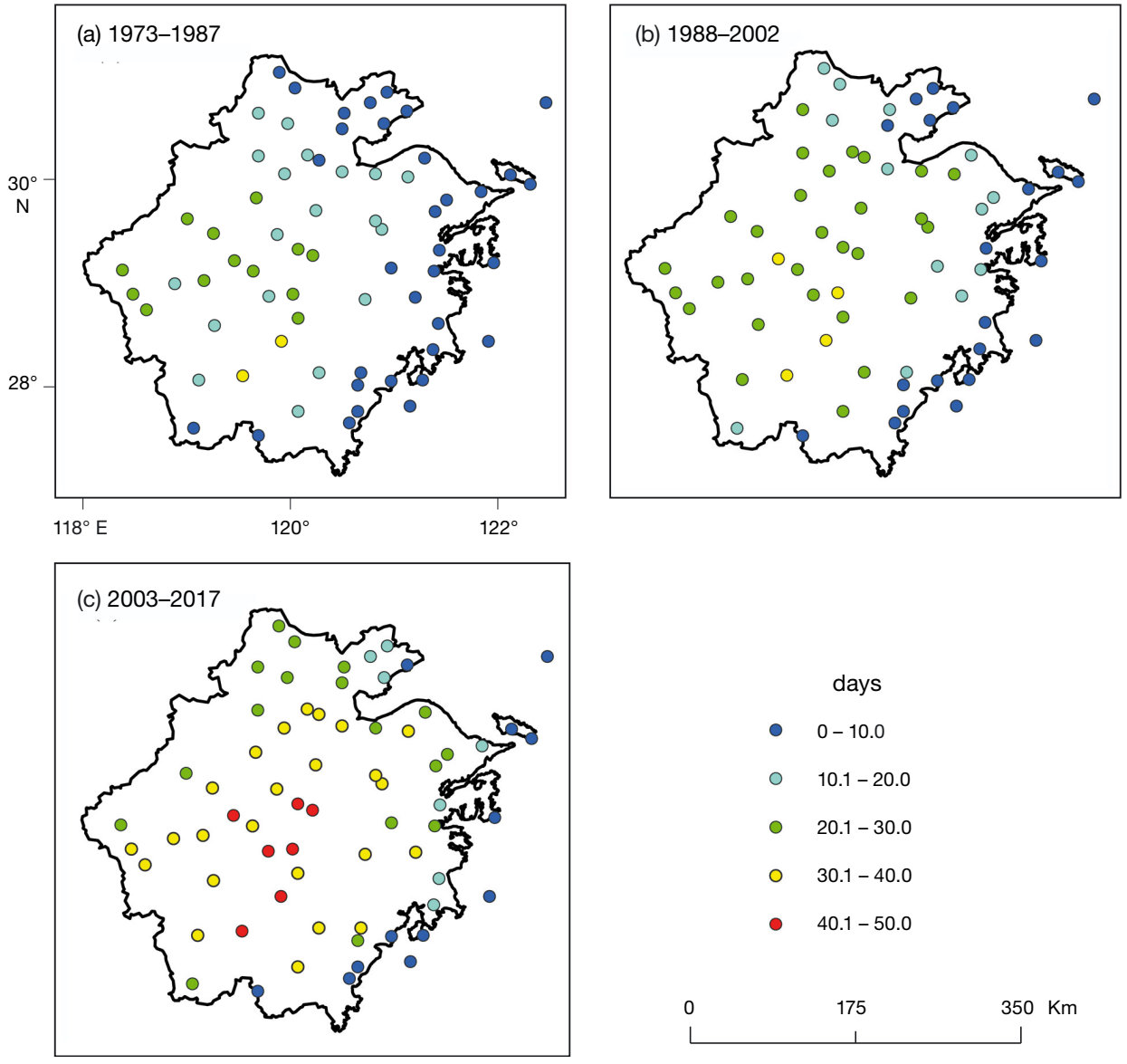

Fig. 6. Heat wave duration (HWD) average values recorded for the periods (a) 1973–1987, (b) 1988–2002, and (c) 2003–2017

4. DISCUSSION AND CONCLUDING REMARKS

Since 2003, HWs have become one of the most serious natural disasters in Zhejiang Province, China. The present analysis, based on the CMA definition, considered 35°C as a temperature threshold to define HW events. This is consistent with the Chinese public's understanding of high temperature and HWs. The AHHT is a comprehensive disaster index for a HW, and is useful to quantify its magnitude in terms of duration and intensity of the induced heat-stress conditions. Temporal and spatial variations of HWs are consistent with those of heat injury to tea plants and early-season rice plants in Zhejiang (Fan et al. 2018, Lou et al. 2018) and with high temperature and drought in summer (Lou et al. 2017).

Generally, we found pronounced decadal variability among the HW magnitude levels. The YAHHT and HWD in 2003–2017 were higher than those in 1973–1987 and 1988–2002. From a synoptic perspective, the intensity and duration of HWs are closely correlated with the western Pacific subtropical high (WPSH) (Wang et al. 2016). In 2013, from 2 July to 19 August, the east of China was under the control of a

Table 2. Recurrence probabilities of the 2003 and 2013 heat waves in Hangzhou, Ningbo, Quzhou, Lishui, and Wenzhou for the present climate (last column) and for 2 previous periods. YAHHT: yearly accumulated harmful high temperature

Station	Year	YAHHT (°C)	1973–1987 (%)	1988–2002 (%)	2003–2017 (%)
Hangzhou	2003	371.5	0.0	0.0	18.7
	2013	754.4	0.0	0.0	3.4
Ningbo	2003	391.5	0.0	0.0	16.4
	2013	596.3	0.0	0.0	3.5
Quzhou	2003	454.8	0.0	0.0	9.1
	2013	510.6	0.0	0.0	4.4
Lishui	2003	886.7	0.0	0.0	3.3
	2013	735.9	0.0	0.0	10.2
Wenzhou	2003	173.8	0.0	0.0	7.2
	2013	167.7	0.0	0.0	9.5

strong and stable WPSH, leading to persistent hot weather in the region (Peng 2014). Contrary to the extremely hot summer of 2013, the 1999 summer was characterized by the occurrence of an extreme La Niña event, which promoted an eastward shift and a continuous weakening of the anticyclonic anomaly system associated with the WPSH. The displacement of this meso-scale atmospheric system towards the interior Pacific Ocean induced a synoptic scenario at the surface and over Zhejiang Province, dominated by southwesterly airflow from the Bay of Bengal and the tropical Indian Ocean, and leading to pronounced rainy and relatively cold conditions.

Since the 1980s, Zhejiang's economy has been developing rapidly with the support of the Chinese economy. Consequently, the gross domestic product (GDP) and NAP levels have increased constantly. After a housing system reform in 1998, many people entered the cities from rural areas to buy houses and engage in nonagricultural work, which promoted the rapid growth of the GDP and NAP after 2000 (Wu & Yang 2018) (Fig. 7). Industrialization, real estate development, and population growth have promoted rapid and intense urbanization in cities, enhancing the urban heat island effect (Yokobori & Ohta 2009, Hao et al. 2015). Since 2000, the scale of cities has continuously increased and urban heat island effects have strengthened HWs (Li & Bou-Zeid 2013). The correlation coefficients between *Ci* and the GDP and NAP were respectively 0.5131 and 0.6005, with correlations reaching a significance level of 0.01.The HW duration and intensity at stations in areas of the province having the fastest-growing economy (e.g. Hangzhou, Shaoxing, Wenzhou, Ningbo, Linhai, and Jinhua) had a strong positive change in the past 45 yr, mainly owing to increased persistence of the YAHHT, but also accompanied by increases in the HWD. The time-variation periodicity of the 8 yr moving average of *Ci* was consistent with those of the GDP and NAP. We found an increase of *Ci* values, particularly after the years 1987 and 2002, and a correspondent increase of GDP and NAP values (Fig. 7).

Focusing on individual stations, geographical conditions strongly affect the intensities of HWs. The stations of central Zhejiang, located in a more interior land region and within basins where heat readily accumulates, are more prone to severe HWs with a higher strength and longer duration (e.g. Lishui station located in the Lishui Basin, Xinchang station located in the Xinsheng Basin, and Jinhua and Lanqi stations located in the Jinqu Basin). Lehner & Whiteman (2012, 2014) used the Weather Research and Forecasting model to perform large-eddy simulations of thermally driven cross-basin winds in idealized, closed basins. In basins 5–10 km wide and 150–300 m deep from the floor to the basin rim, cross-basin temperature differences that were representative of east- and west-facing slopes were insufficient to maintain perceptible cross-basin winds. The thermal circulation was very weak (small eddy)

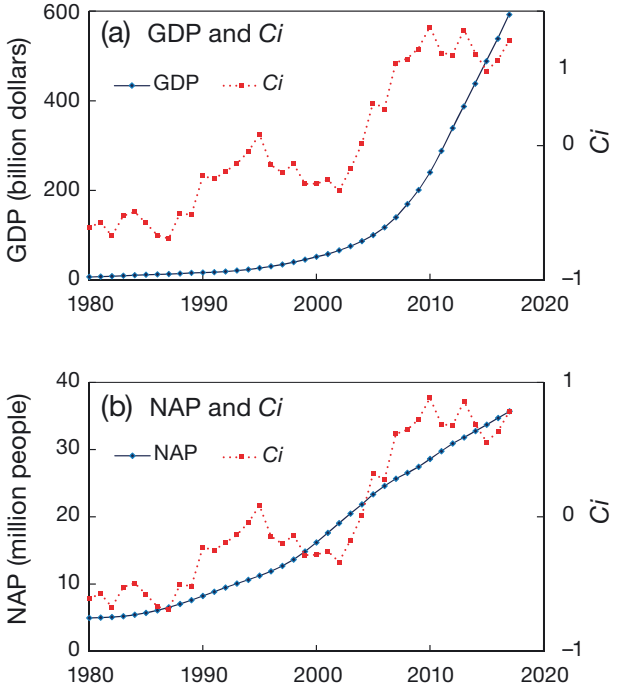

Fig. 7. 8 yr moving average time series of (a) the comprehensive index of hot summer severity (*Ci*) and gross domestic product (GDP) and (b) *Ci* and the non-agricultural population index (NAP) in Zhejiang from 1973–2017

or was even nonexistent, and heat was easily accumulated in the basin. Thus, although Lishui station is classified as an MCS, it presented the highest HW intensity in Zhejiang because of its location within the smaller Lishui Basin. Stations located on small islands (i.e. Dachen, Yuhuan, and Tongtou) recorded a low number of HWs and observed low values of the YAHHT and HWD indices, due to their proximity to the ocean and to high levels of vegetation. Both factors together contribute to smoothen the variability, as well as the absolute values of temperature. Therefore, over these particular regions, we are unlikely to observe single and consecutive days with temperature values >35°C, which, using the HW definition adopted in this study, makes it impossible to identify HW episodes. No significant HW trend values were recorded for stations located on large islands (i.e. Shengsi and Putou), on the coast (i.e. Shipu and Leqin), or in mountain areas with high forest coverage (i.e. Kaihua, Chunan, and Taishun).

The recurrence probabilities of the most and second-most severe HWs of Zhejiang in Ningbo, Lishui, Quzhou, Hangzhou, and Wenzhou — which occurred in 2013 and 2003, respectively — were estimated using an information diffusion model. Results show that the recurrence probability of such a severe hot summer has been low in the past climate, but is high in the present climate. The recurrence probability of a hot summer similar to or exceeding the July–September 2003 hot summer is once every 5–7 yr in Hangzhou and Ningbo and once every 11 yr in Quzhou. The recurrence probability of hot summers similar to or exceeding the July–August 2013 hot summer is once every 10 yr in Lishui. The recurrence probability of a hot summer similar to or exceeding the 2003 and 2013 hot summer is once every 10–14 yr in Wenzhou. These results should be considered in the design of adaptation and mitigation measures that protect society against the adverse effects of severe HWs.

Acknowledgements. This paper was financially supported by the Science Technology Department of Zhejiang Province, China (No. LGN18D050001). We thank Glenn Pennycook, MSc, from LiwenBianji, Edanz Group China (www.liwenbianji.cn/ac), for editing the English text of a draft of this manuscript.

LITERATURE CITED

Changnon D, Sandstrom M, Schaffer C (2003) Relating changes in agricultural practices to increasing dew points in extreme Chicago heat waves. Clim Res 24:243–254

Ding T, Ke Z (2015) Characteristics and changes of regional wet and dry heat wave events in China during 1960–2013. Theor Appl Climatol 122:651–665

Fan H, Lv P, Wang P, Hu T and others (2018) Assessment of heat-injury-risk spatial difference for early rice in Zhejiang Province under global warming. J Hangzhou Norm Univ 17:326–331 (in Chinese)

Feng L, Xiong W, Ju H, Cao Y, Yang D (2015) Changes of high temperature events during rice growth period in MLRYR under RCP scenarios. Chin J Agrometeorol 36: 383–392 (in Chinese)

Feng M, Liu A, Wu Y, Hu Y, Zhang F (2008) Temperature index of high temperature harm for main crops (GB/T 21985-2008). General Administration of Quality Supervision, Inspection and Quarantine of the P. R. C. Beijing (in Chinese)

Gross MH, Alexander LV, Macadam I, Geen D, Evans JP (2017) The representation of health relevant heatwave characteristics in a regional climate model ensemble for New South Wales and the Australian Capital Territory, Australia. Int J Climatol 37:1195–1210

Hao L, Sun G, Liu Y, Wan J and others (2015) Urbanization dramatically altered the water balances of a paddy field-dominated basin in southern china. Hydrol Earth Syst Sci 19:3319–3331

Hellebrekers LJ, de Boer EJ, van Zuylen MA, Vosmeer H (1997) A comparison between medetomidine-ketamine and medetomidine-propofol anaesthesia in rabbits. Lab Anim 31:58–69

Huang C (1997) Principle of information diffusion. Fuzzy Sets Syst 91:69–90

Huang C (2002) Information diffusion techniques and small-sample problem. Int J Inf Technol Decis Making 1:229–249

Huynen M, Marten P, Schrambijkerk D, Weijenberg MP, Kunst AE (2001) The impacts of heat waves and cold spells on mortality rates in the Dutch population. Environ Health Perspect 109:463–470

IPCC (2014) Climate change 2013: the physical science basis. Contribution of Working Group I to the Fifth Assessment Report of the Intergovernmental Panel on Climate Change. https://www.ipcc.ch/report/ar5/wg1/

Jiang T, Zhao J, Cao L, Wang Y and others (2018) Projection of national and provincial economy under the shared socioeconomic pathways in China. Clim Change Res 14: 50–58 (in Chinese)

Lee JS, Byun HR, Kim DW (2016) Development of accumulated heat stress index based on time-weighted function. Theor Appl Climatol 124:541–554

Lee TW, Ho A (2010) Scaling of the urban heat island effect based on the energy balance: nighttime minimum temperature increase vs. urban area length scale. Clim Res 42:209–216

Lehner M, Whiteman CD (2012) The thermally driven cross-basin circulation in idealized basins under varying wind conditions. J Appl Meteorol Climatol 51:1026–1045

Lehner M, Whiteman CD (2014) Physical mechanisms of the thermally driven cross-basin circulation. QJR Meteorol Soc 140:895–907

Li D, Bou-Zeid E (2013) Synergistic interactions between urban heat islands and heat waves: the impact in cities is larger than the sum of its parts. J Appl Meteorol Climatol 52:2051–2064

Liu L, Xu ZX (2016) Regionalization of precipitation and the spatiotemporal distribution of extreme precipitation in southwestern China. Nat Hazards 80:1195–1211

Lou W, Wu L, Chen H, Mao Y (2010) Analysis and design of premium rates determined for weather-based index insurance contract of citrus. Zhongguo Nong Ye Ke Xue 43:1904–1911 (in Chinese)

Lou W, Sun S, Sun K, Yang X, Li S (2017) Summer drought index using SPEI based on 10-day temperature and precipitation data and its application in Zhejiang Province (Southeast China). Stochastic Environ Res Risk Assess 31:2499–2512

Lou W, Xiao Q, Sun K, Deng S, Yang M (2018) Heat injure risk regionalization of tea plant in Zhejiang Province. Chaye Kexue 38:553–562 (in Chinese)

Nogueira P, Paixão E (2008) Models for mortality associated with heatwaves: update of the Portuguese heat health warning system. Int J Climatol 28:545–562

Peng J (2014) An investigation of the formation of the heat wave in southern China in summer 2013 and the relevant abnormal subtropical high activities. Atmos Ocean Sci Lett 7:286–290

Peres LF, de Lucena AJ, Rotunno Filho OC, de Almeida França JR (2018) The urban heat island in Rio de Janeiro, Brazil, in the last 30 years using remote sensing data. Int J Appl Earth Obs Geoinf 64:104–116

Perkins SE (2015) A review on the scientific understanding of heatwaves — their measurement, driving mechanisms, and changes at the global scale. Atmos Res 164-165:242–267

Perkins SE, Alexander LV (2013) On the measurement of heat waves. J Clim 26:4500–4517

Prasad PVV, Jagadish SVK (2017) Field crops and the fear of heat stress–opportunities, challenges and future directions. Field Crops Res 200:114–121

Raggad B (2018) Statistical assessment of changes in extreme maximum temperatures over Saudi Arabia, 1985–2014. Theor Appl Climatol 132:1217–1235

Ren F, Cui D, Gong Z, Wang Y and others (2012) An objective identification technique for regional extreme events. J Clim 25:7015–7027

Roldán E, Gómez M, Pino MR, Pórtoles J, Linares C, Díaz J (2016) The effect of climate-change-related heat waves on mortality in Spain: uncertainties in health on a local scale. Stochastic Environ Res Risk Assess 30:831–839

Russo S, Dosio A, Graversen RG, Sillmann J and others (2015) Magnitude of extreme heat waves in present climate and their projection in a warming world. J Geophys Res Atmos 119:500–512

Savić S, Selakov A, Milošević D (2014) Cold and warm air temperature spells during the winter and summer seasons and their impact on energy consumption in urban areas. Nat Hazards 73:373–387

Sen PK (1968) Estimates of the regression coefficient based on Kendall's tau. J Am Stat Assoc 63:1379–1389

Shadmani M, Roknian M (2012) Trend analysis in reference evapotranspiration using Mann-Kendall and Spearman's rho tests in arid regions of Iran. Water Resour Manag 26: 211–224

Shou Y, Zhang D (2012) Recent advances in understanding urban heat island effects with some future prospects. Acta Meteorol Sin 70:338–353 (in Chinese)

Siegle MR, Taylor EB, O'Connor MI (2018) Prior heat accumulation reduces survival during subsequent experimental heat waves. J Exp Mar Biol Ecol 501:109–117

Smith TT, Zaitchik BF, Gohlke JM (2013) Heat waves in the United States: definitions, patterns and trends. Clim Change 118:811–829

Spinoni J, Lakatos M, Szentimrey T, Bihari Z, Szalai S, Vogt J, Antofie T (2015) Heat and cold waves trends in the Carpathian region from 1961 to 2010. Int J Climatol 35: 4197–4209

Sun Y, Zhang X, Zwiers FW, Song L and others (2014) Rapid increase in the risk of extreme summer heat in eastern China. Nat Clim Chang 4:1082–1085

Tan J, Huang J (2004) The impacts of heat waves on human health and its research methods. Clim Environ Res 9: 680–686 (in Chinese)

Unal YS, Tan E, Mentes SS (2013) Summer heat waves over western Turkey between 1965 and 2006. Theor Appl Climatol 112:339–350

Wang W, Zhou W, Li X, Wang X, Wang D (2016) Synoptic-scale characteristics and atmospheric controls of summer heat waves in China. Clim Dyn 46:2923–2941

WMO, WHO (2015) Heat waves and health: guidance on warning-system development. Rep 1142. WMO, Geneva

Wu B, Yang C (2018) Housing system, ensuring people's access to housing and regulation over the years: observation from the Central Government Work Reports from 1978 to 2017. Reform 287:74–85 (in Chinese)

Xia J, Tu K, Yan Z, Qi Y (2016) The super-heat wave in eastern China during July–August 2013: a perspective of climate change. Int J Climatol 36:1291–1298

Xie Y (2017) Practical questions and answers on high temperature allowance. Hum Resour 09:57–59 (in Chinese)

Xu J, Deng Z, Chen M (2009) A summary of studying on characteristics of high temperature and heat wave damage in China. J Arid Meteorol 27:163–167 (in Chinese)

Yang X, Hou Y, Chen B (2011) Observed surface warming induced by urbanization in east China. J Geophys Res 116:D14113

Ye D, Yin J, Chen Z, Zheng Y and others (2013) Spatiotemporal change characteristics of summer heatwaves in China in 1961-2010. Clim Change Res 9:15–20 (in Chinese)

Yokobori T, Ohta S (2009) Effect of land cover on air temperatures involved in the development of an intra-urban heat island. Clim Res 39:61–73

Zhang P, Guo L (1999) Zhejiang climate and its application. China Meteorological Press, Beijing (in Chinese)

Appendix. Station information

Table A1. Stations used in the present study. MCS: medium-sized-city station, SCS: small-city station, MES: metropolitan station, LCS: large-city station, DCS: distance of continental station from the sea

Station ID	Name	Latitude (°S)	Longitude (°E)	Elevation (m)	Type	DCS (km)
1	Changxin	31.02	119.9	25	MCS	100.29
2	Huzhou	30.87	120.05	4.1	MCS	78.46
3	Jiashan	30.83	120.93	2.6	MCS	28.77

Table A1 (continued)

Station ID	Name	Latitude (°S)	Longitude (°E)	Elevation (m)	Type	DCS (km)
4	Shengsi	30.73	122.45	79.6	SCS	Island
5	Jiaxing	30.73	120.77	4.8	MCS	28.32
6	Pinghu	30.65	121.12	4	MCS	3.4
7	Anjie	30.63	119.7	72.2	SCS	92.07
8	Deqin	30.53	119.98	102	MCS	63.33
9	Tongxiang	30.63	120.52	6	MCS	29.15
10	Haiyan	30.53	120.9	4.8	MCS	5.06
11	Haining	30.48	120.5	5.3	MCS	17.78
12	Hangzhou	30.23	120.17	43.2	MES	43.4
13	Xiaoshan	30.18	120.28	96.5	MCS	34.04
14	Linan	30.22	119.7	117.6	SCS	87.77
15	Fuyang	30.05	119.95	47.9	MCS	66.76
16	Shaoxing	30.07	120.5	7.9	LCS	15.63
17	Shangyu	30.05	120.82	6.4	MCS	8.43
18	Cixi	30.2	121.29	5.7	MCS	12.14
19	Yuyao	30.02	121.13	38	MCS	24.44
20	Dinghai	30.04	122.11	35.7	MCS	Island
21	Putou	29.95	122.3	85.2	SCS	Island
22	Tonglu	29.82	119.68	44.8	SCS	98.54
23	Zhuji	29.7	120.25	39.1	MCS	61.82
24	Shengzhou	29.6	120.82	104.3	MCS	58.88
25	Xinchang	29.52	120.88	115.1	SCS	52.67
26	Ningbo	29.8	121.5	6.2	MES	25.76
27	Beilen	29.88	121.83	5	MCS	5.61
28	Fenghua	29.69	121.39	41.5	SCS	18.93
29	Ninghai	29.32	121.43	25	SCS	9.84
30	Shipu	29.2	121.95	129.2	SCS	Island
31	Chunan	29.62	119.02	172.2	SCS	165.51
32	Jiande	29.48	119.27	87.2	MCS	150.54
33	Pujiang	29.47	119.88	85.2	SCS	104.55
34	Yiwu	29.33	120.08	90	MCS	105.4
35	Dongyang	29.27	120.22	91.9	MCS	105.4
36	Lanxi	29.22	119.47	48.3	MCS	152.31
37	Jinhua	29.12	119.65	64.7	MCS	148.55
38	Wuyi	28.88	119.8	103.8	SCS	136.36
39	Yongkuang	28.9	120.03	102.9	SCS	118.46
40	Tiantai	29.15	120.97	107.6	SCS	43.27
41	Shanmen	29.12	121.38	34.5	SCS	5.36
42	Xianju	28.85	120.72	83	SCS	68.12
43	Linhai	28.87	121.2	6.6	MCS	31.34
44	Hongjia	28.62	121.42	4.6	MCS	8.86
45	Dachendao	28.45	121.9	86.2	SCS	Island
46	Wenlin	28.37	121.37	35.3	MCS	7.38
47	Kaihua	29.13	118.4	153.6	SCS	242.69
48	Quzhou	29	118.9	82.4	MCS	210.17
49	Longyou	29.03	119.18	66.2	SCS	187.29
50	Changshan	28.9	118.5	137	SCS	247.16
51	Jiangshan	28.75	118.63	126.3	SCS	229.05
52	Suichang	28.6	119.28	238.6	SCS	164.57
53	Jinyun	28.67	120.08	179.1	SCS	101.69
54	Lishui	28.45	119.92	59.7	MCS	153.49
55	Longquan	28.08	119.13	222.1	SCS	153.49
56	Yunhuo	28.12	119.55	159.6	SCS	110.65
57	Qintian	28.15	120.28	57.8	SCS	55.43
58	Yongjia	28.15	120.68	34.3	SCS	22.82
59	Wenzhou	28.03	120.65	28.3	LCS	16.95
60	Leqin	28.07	120.97	60.8	MCS	2.1
61	Yuhuan	28.08	121.27	95.9	SCS	Island
62	Qinyuan	27.62	119.08	400.8	SCS	140.05
63	Taishun	27.55	119.7	538.9	SCS	81.12
64	Wencheng	27.78	120.08	105.4	SCS	54.86
65	Ruian	27.78	120.65	39.7	MCS	8.85
66	Tongtuo	27.83	121.15	68.6	MCS	Island
67	Pingyang	27.67	120.57	254	SCS	8.78

Editorial responsibility: Ricardo Trigo, Lisbon, Portugal

Submitted: August 23, 2018; Accepted: August 27, 2019
Proofs received from author(s): November 5, 2019